Journal of Marine Systems 83 (2010) 1–13

Contents lists available at ScienceDirect

Journal of Marine Systems

journal homepage: www.elsevier.com/locate/jmarsys

Coastal upwelling in the South Atlantic Bight: A revisit of the 2003 cold event using long term observations and model hindcast solutions

Kyung Hoon Hyun, Ruoying He *

Department of Marine, Earth and Atmospheric Sciences, North Carolina State University, North Carolina, USA 27695

ARTICLE INFO

Article history:
Received 29 September 2009
Received in revised form 18 May 2010
Accepted 25 May 2010
Available online 6 August 2010

Keywords:
South Atlantic Bight coastal circulation
Observation and modeling
Gulf stream

ABSTRACT

Long-term (2002–2008) buoy observations, satellite imagery, and regional ocean circulation hindcast solutions were used to investigate the South Atlantic Bight (SAB) cold event that occurred in summer 2003. Observations confirmed that SAB shelf water temperature during the event was significantly colder than their 7-year (2002–2008) mean states. The cold event consisted of 6 distinctive cold wakes, which were likely related with intra-seasonal oscillations in wind fields. The upwelling index analyses based on both in situ buoy wind and North American Regional Reanalysis (NARR) highlighted that the upwelling favorable winds in 2003 were the strongest and most persistent over the 7-year study period. The regional circulation model hindcast driven by the large scale data assimilative model, NARR surface meteorological forcing and coastal river runoff generally reproduced observed hydrodynamic variability during the event. Further model analyses revealed a close relationship between the cold bottom water intrusion and the Gulf Stream (GS) core intensity and its position relative to the shelf break. Being more intensive and shoreward located, the GS worked in concert with strong upwelling favorable wind field to produce abnormal upwelling in summer 2003.

1. Introduction

The South Atlantic Bight (SAB) stretches from Cape Canaveral, Florida, to Cape Hatteras, North Carolina, covering ~700 km of the seaboard of U.S. southeast coastal ocean. Shelf-widths are at a maximum in the central SAB off the coast of Georgia, reaching approximately 120 km offshore. Off Cape Canaveral and Cape Hatteras, shelf-widths are at a minimum, being only about 10–30 km. A topographic ridge known as the Charleston Bump is present at 32° N off the coast of Charleston, South Carolina. Distinct circulation dynamic regimes generally subdivide the SAB into the inner shelf (~0–20 m), middle shelf (~20–40 m), outer shelf (~40–70 m) and shelf slope (~70–200 m) (Atkinson and Menzel, 1985). Circulation in the inner shelf and mid shelf is largely driven by river runoff, local wind and Gulf Stream (GS) frontal activities, whereas the outer shelf and continental slope are primarily forced by the Gulf Stream (Lee et al. 1981, 1991; Lee and Atkinson, 1983; Atkinson et al., 1987). Early field experiment studies on the SAB circulation, including GABEX I, II (Georgia Bight Experiment: Lee and Atkinson, 1983), GALE (Genesis of Atlantic Lows Experiments; Blanton et al., 1989), and FLEX (the 1987 Fall Experiment; Werner et al., 1993) have accumulated in situ hydrographic and biological data that have helped to significantly improve the understanding of SAB shelf circulation and coastal ecosystem responses to both local forcing and deep-ocean forcing. Blanton et al. (2003a,b) based on accumulated temperature and salinity observations from 1955 to 1999 and wind data from 1975 to 1999, further presented the monthly mean hydrographic climatology for the SAB.

Topographic effects on the regional circulation was investigated by Janowitz and Pietrafesa (1982), which showed that the divergent isobaths in the northeastern Florida shelf can significantly enhance local upwelling. Downstream, the Charleston Bump (CB) effect was a topic of many studies (e.g., Pietrafesa et al., 1978; Rooney et al., 1978; Brooks and Bane, 1978; Chao and Janowitz, 1979; Dewar and Bane, 1985; Xie et al., 2007), which showed that the CB was responsible for large GS meanders and filaments, and its isobathic curvature provided a localized mechanism to maximize GS baroclinic and barotropic energy transfer.

On the event scale, previous studies (e.g., Blanton et al., 1981; Hofmann, 1981; Klinck et al., 1981; Atkinson, 1985; Lee and Pietrafesa, 1987; Hamilton, 1987) showed that the cold water intrusions (hereafter, cold water intrusion, GS intrusion, bottom intrusion, and cold water upwelling are interchangeable and used for the same meaning) could be resulted from wind, GS proximity to the shelf break, and GS frontal eddy activities. Intrusions took place when upwelling favorable winds were observed at times when the GS was also in a relatively onshore position. Specific GS influence on the SAB has been examined by Lee and Atkinson (1983) and Lee et al. (1985, 1991), among others. These studies suggested that low frequency current and temperature variability at the shelf break were produced by cyclonic, cold-core GS frontal eddies. The GS effect can often be

* Corresponding author. Tel.: +1 919 512 249.
E-mail address: rhe@ncsu.edu (R. He).

0924-7963/$ – see front matter © 2010 Elsevier B.V. All rights reserved.
doi:10.1016/j.jmarsys.2010.05.014

identified on the mid shelf, and sometimes even on the inner shelf of the SAB. Using satellite imagery and moored current and temperature records, these studies also confirmed that the GS meanders and eddies were persistent features between Miami and Cape Hatteras, and that the GS frontal eddies served as a deep-ocean "nutrient pump" for the SAB shelf ecosystem.

One significant example of such cold water intrusions occurred in summer, 2003. Observations and simulations of the anomalous hydrographic conditions in the central SAB during spring and summer of 2003 were reported by Aretxabaleta et al. (2006; 2007). Using satellite data and coastal observations, Yuan (2006) also reported the important role of the strong and persistent southwesterly winds in this cold event. Recently, Miles et al. (2009) reconstructed SAB daily cloud-free SST and chlorophyll-a using the Data Interpolating Empirical Orthogonal Function (DINEOF) method for 2003. The second EOF mode in the reconstructed DINEOF SST showed a clear linkage between upwelling winds and the abrupt SST drop near the coast. The large scale atmospheric forcing condition in 2003 was studied by Schwing and Pickett (2004), which indicated a teleconnection between the global atmospheric system and regional wind pattern off the U.S. east coast. Using long-term satellite observations, Signorini and McClain (2007) suggested that the seasonal variability of the North Atlantic Subtropical Gyre (NASG), which expands in summer and contracts in winter, can drive excursions of the GS on and off the SAB shelf. Therefore, it is possible for the boundary current variations (i.e., the intensity of the GS and its proximity to the shelf) to work in conjunction with local wind forcing anomaly to produce strong coastal upwelling, an important question deserving further study.

The goal of this paper is to revisit the 2003 cold water event in the context of long-term observations and numerical model hindcast solutions. We examined the relative contributions of local wind forcing and deep-ocean GS forcing in causing such a significant upwelling event. We utilized long-term (2002–2008) wind and temperature data from the National Data Buoy Center, daily, cloud-free DINOEOF satellite SST (Miles et al., 2009), and circulation hindcast from a regional ocean model. Two sensitivity model experiments with and without wind forcing were carried out to investigate the effects of wind and GS independently.

2. Data and model

Buoy measured surface temperature and wind time series were obtained from the National Data Buoy Center (NDBC) for this study. Four buoys in the SAB were chosen (Fig. 1b) and their daily mean values were computed based on hourly observations. Upwelling indices (*UI*, i.e., the offshore component of the Ekman transport) were then calculated from buoy winds following the method of Schwing et al. (1996), i.e. $UI = \tau / f$, where τ is the alongshore wind stress calculated using the method of Large and Pond (1981) and f is the local Coriolis parameter. We used *UI* in this study as a proxy of the intensity of upwelling favorable wind. In addition, the time series of cable-derived volume transport through the Florida Straits was obtained from www.aoml.noaa.gov to quantify the intensity of the GS and to compare with model simulated GS transport. Daily, cloud-free satellite SST reconstructions were used to examine the temporal and spatial distributions of upwelled cold waters in the SAB. Miles et al. (2009) provided details on how such daily reconstructions were obtained using the Data interpolating Empirical Orthogonal Function (DINEOF) method.

The circulation hindcast model was implemented based on the Regional Ocean Modeling System (ROMS, Haidvogel et al., 2008; Shchepetkin and McWilliams, 2005). The model domain encompasses the entire Gulf of Mexico and South Atlantic Bight (hereafter SABGOM ROMS) as depicted in Fig. 1a. Its spatial resolution is ~5 km and vertically 36 layers are weighted to better resolve surface and bottom boundary layers. For open boundary conditions, SABGOM ROMS is one-way nested inside the 1/12° data assimilative North Atlantic Hybrid Coordinate Ocean Model (DA HYCOM, Chassignet et al., 2003).

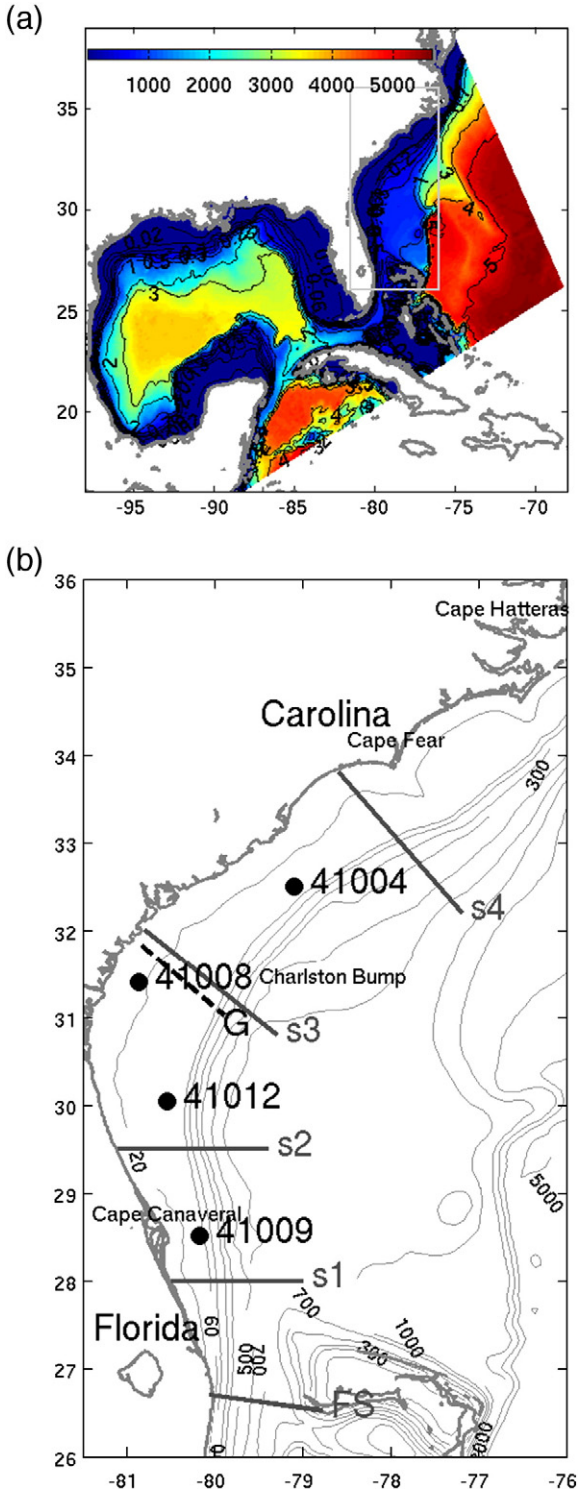

Fig. 1. (a) The domain and bathymetry of the South Atlantic Bight and the Gulf of Mexico (SABBOM) circulation model (color bar in meters) and (b) the locations of National Data Buoy Center (NDBC) buoys (solid circle) and sections. Cross-shelf sections (s1–s4) are used to demonstrate the cold water intrusion (Figs. 12 and 13), section FS is used to calculate Gulf Stream volume transport through the Florida Straits (Fig. 10), and section G for model-data comparison (Fig. 11). The water depths at buoy 41008, 41012, 41009 and 41004 are 18 m, 38 m, 42 m and 34 m, respectively.

During the SABGOM ROMS hindcast, we relaxed the model interior temperature and salinity fields to their HYCOM counterparts with a time scale of 20 days. Such a relaxation provided an efficient way to constrain the regional ROMS solutions with the large scale, data assimilative HYCOM solutions. Tidal forcing was neglected in our ROMS simulation as the subtidal circulation is considered the most relevant dynamic process of this summer-long cold event. A caveat we note is during certain conditions, tidal mixing can be one of the dominant factors controlling the hydrographic vertical structure over the SAB shelf (Blanton et al., 2004). Major coastal river input in the SABGOM was included in the hindcast using daily runoff data observed by USGS river gauges along the coast. For both momentum and buoyancy forcing at the model surface, we utilized three hourly, 32-km horizontal resolution North American Regional Reanalysis (NARR, www.cdc.noaa.gov). Two model experiments were carried out with and without the NARR wind forcing to examine the effects of local wind and the GS, respectively. We also used the numerical particle tracking embedded in the ROMS simulation to examine the GS intrusion and upwelling intensity over the SAB continental slope.

Our model hindcast simulations ran from June 2003 to December 2007, providing the long-term model realizations of SAB coastal hydrography, transport, variability of the GS position and core intensity. For the purpose of this study, we focused on the model results from June to September, 2003 to examine the evolution of the 2003 summer cold event.

3. Results

3.1. Temperature

NDBC buoy measured surface temperature time series indicated that the shelf waters in summer 2003 were indeed much colder than their long-term (7 years, 2002–2008) means (Fig. 2). For example at buoys 41008, 41012 and 41009, cold temperature anomalies in the central SAB were as big as 4 °C in July and August, significantly larger than 1 standard deviation of their respective mean temperature values. These temperature time series also highlighted that the summer 2003 cold event in fact consisted of 6 cold wakes from June to September 2003, which were most distinctive at buoy 41008 and 41012. These cold wakes were also seen at buoy 41009 and 41004. Table 1 summarizes the duration and temperature anomalies during these cold wakes. The first wake lasted about 4 days with a temperature drop of ~1 °C. Subsequent wakes 2 to 4 took place at an interval of 1–2 weeks. The 5th wake presented the largest temperature drop (−4 °C) with the longest duration (9 days). At buoy 41008, water temperature continued its cooling trend after the 6th wake, whereas waters at other buoys (i.e., 41012 and 41009) began to warm up because they are located relatively offshore, thus subject more to the warm GS influence.

Table 1
The dates, durations, the lowest temperature and temperature anomalies of the six cold wakes that occurred in the South Atlantic Bight in summer 2003. Data are based on the surface water temperature measured by NDBC buoy 41008.

Cold wakes	Occurrence (peak)	Duration (days)	Lowest T (°C)	T anomaly (°C)
1st	June 20	4	26.2	−1.0
2nd	July 3	6	26	−2.0
3rd	July 12	7	25	−2.2
4th	July 24	7	24	−2.3
5th	August 12	9	23.8	−4.0
6th	September 8	7	25.1	−3.0

Consecutive cloud-free SST images offered the shelf-wide views of temperature distributions during these six cold wakes (Fig. 3). On 22 June, cold water mass with temperature of ~27 °C appeared near the coastline between 27 and 31°N; then on the next day, this cold water expanded 30–60 km offshore with the temperature value dropped to 25 °C (first cold wake; Fig. 3a–b). Subsequent cold wakes occurred on July 4–5 (2nd; Fig. 3c–d), 10–11(3rd; Fig. 3e–f), 20–22 (4th; Fig. 3g–h), respectively. By July 22, cold water mass had expanded over the entire shelf from the east coast of Florida to the Carolina coast (Fig. 3h). The strength of cold water mass slightly weakened in early

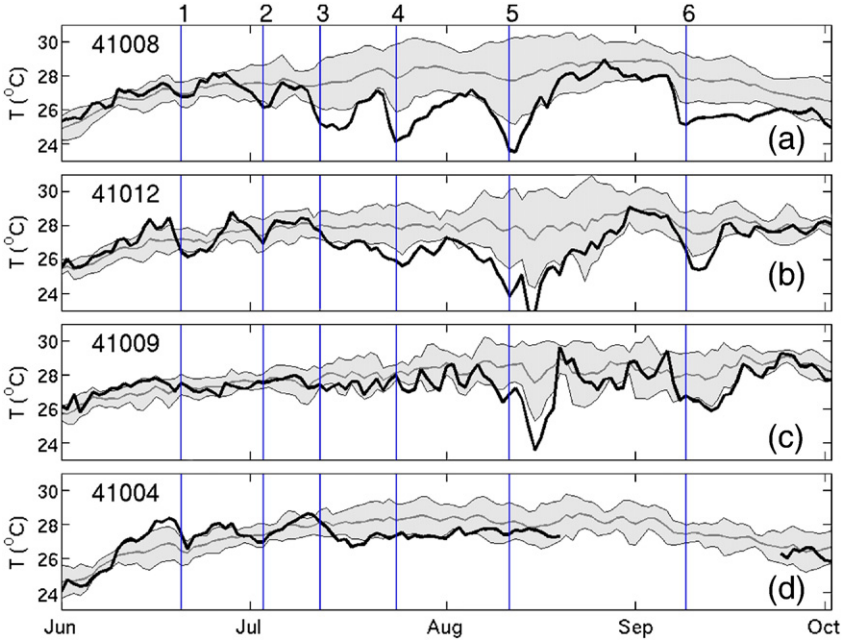

Fig. 2. Time series of buoy-measured water temperature from June to September 2003 at buoy (a) 41008, (b) 41012, (c) 41009 and (d) 41004. Six cold wakes (occurred on June 20, July 3, 12, 24, August 11 and September 8, 2003) are identified with buoy 41008 data and denoted by vertical lines. For each station, the long-term (2002–2008) mean temperature along with its standard deviation envelope are depicted and shaded.

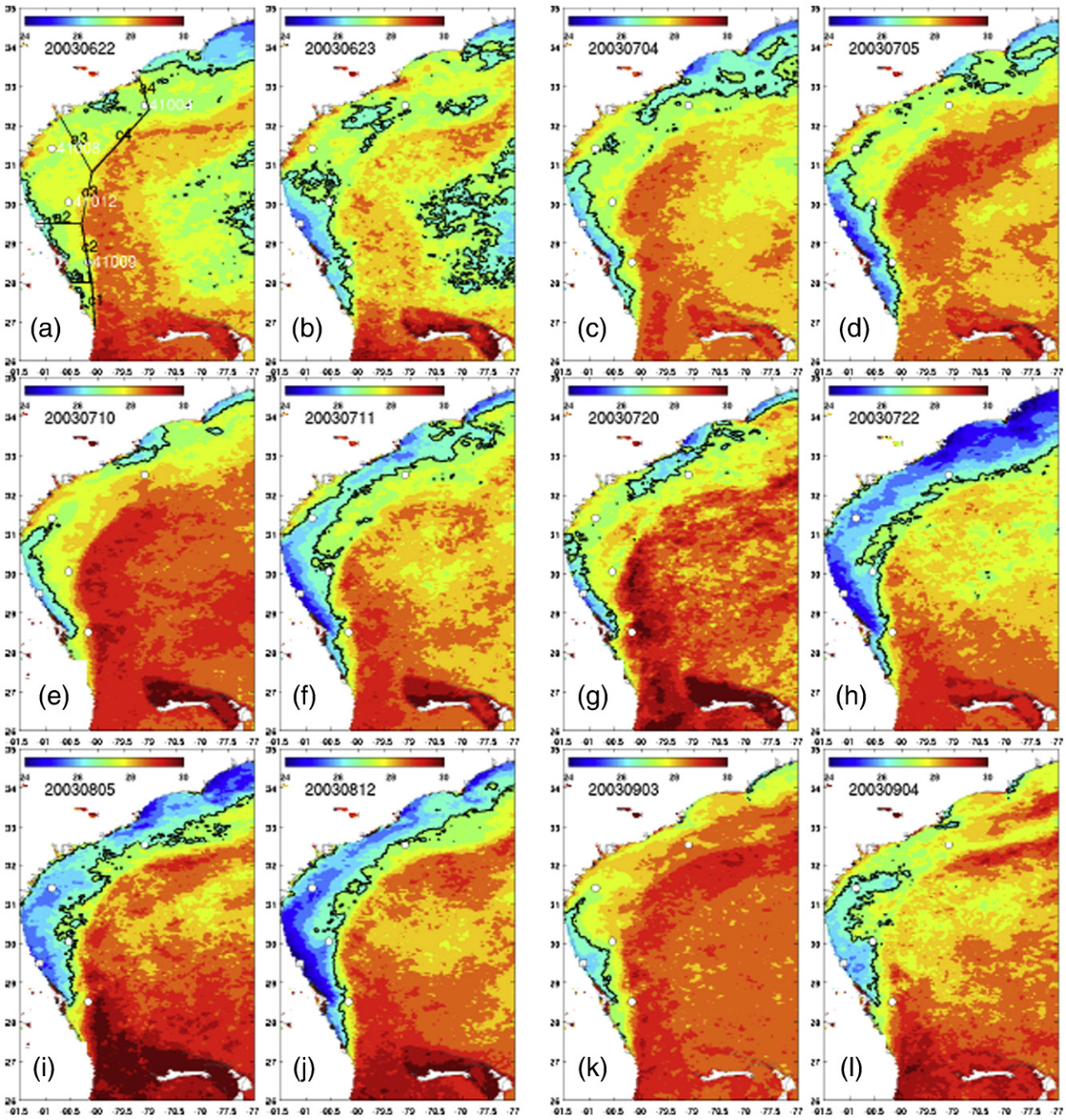

Fig. 3. Satellite derived SST (°C) distribution for the six cold wakes defined in Fig. 2 (from top left to bottom right). The contour of 27 °C (solid black line) is used to demonstrate the expansion of the cold water. Dates are chosen to encompass the beginning and expansion of each cold wake.

August, but strengthened again in mid-August (August 12; 5th wake; Fig. 3i–j). Then there was a relatively weak cold wake that occurred at the beginning of September (6th wake; Fig. 3k–l). For all 6 wakes, the center of cold water was consistently located at 81.1°W/29.5°N near St. Augustine, Florida (denoted by the white square). The time intervals between these 6 cold wakes are 13, 9, 12, 17, 26 days, with the mean being 15 days.

3.2. Wind

The progressive vector diagram (PVD) calculations based on wind observations at buoy 41008 allow us to examine the uniqueness of 2003 upwelling favorable wind in a long-term context (1998–2008). The wind PVD comparisons between 2003 and other years (Fig. 4a) clearly show that the southwesterly winds in summer 2003 were the most persistent over the past 11-year period. The PVDs from other buoys (Fig. 4b) in summer 2003 illustrate the spatial distribution and temporal evolutions of the shelf wind. In general, coastal winds were parallel to the coastline. The speeds of southeasterly/southerly wind started increasing in June, peaked in July and then decreased in August. In addition these point-wise buoy observations, NARR monthly mean wind fields in summer 2003 further provided the large scale spatial views (Fig. 5). The mean upwelling favorable wind conditions dominated in June, July and August. Then the reversal of

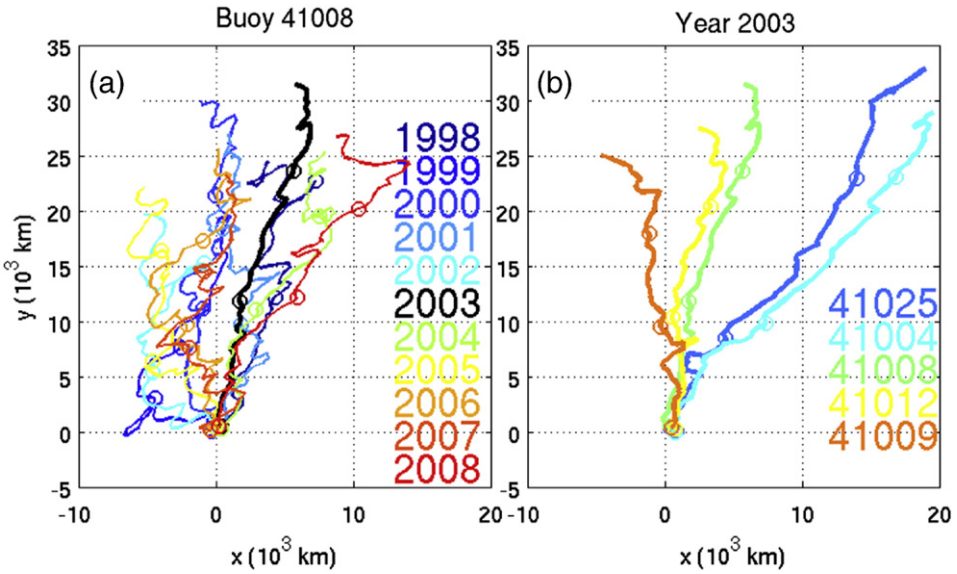

Fig. 4. Progressive vector diagrams calculated based on wind data at (a) buoy 41008 in summer (June–August) of 1998–2008 and (b) five different buoys in the summer of 2003. Daily-averaged wind vector from each buoy is used. Markers indicate the beginnings of June, July and August, respectively. For summer 2003 winds (b), five buoys are chosen to demonstrate wind direction changes at various locations in the SAB. In general, coastal winds were well parallel to the coastline. Buoy 41025 is located off the Cape Hatteras.

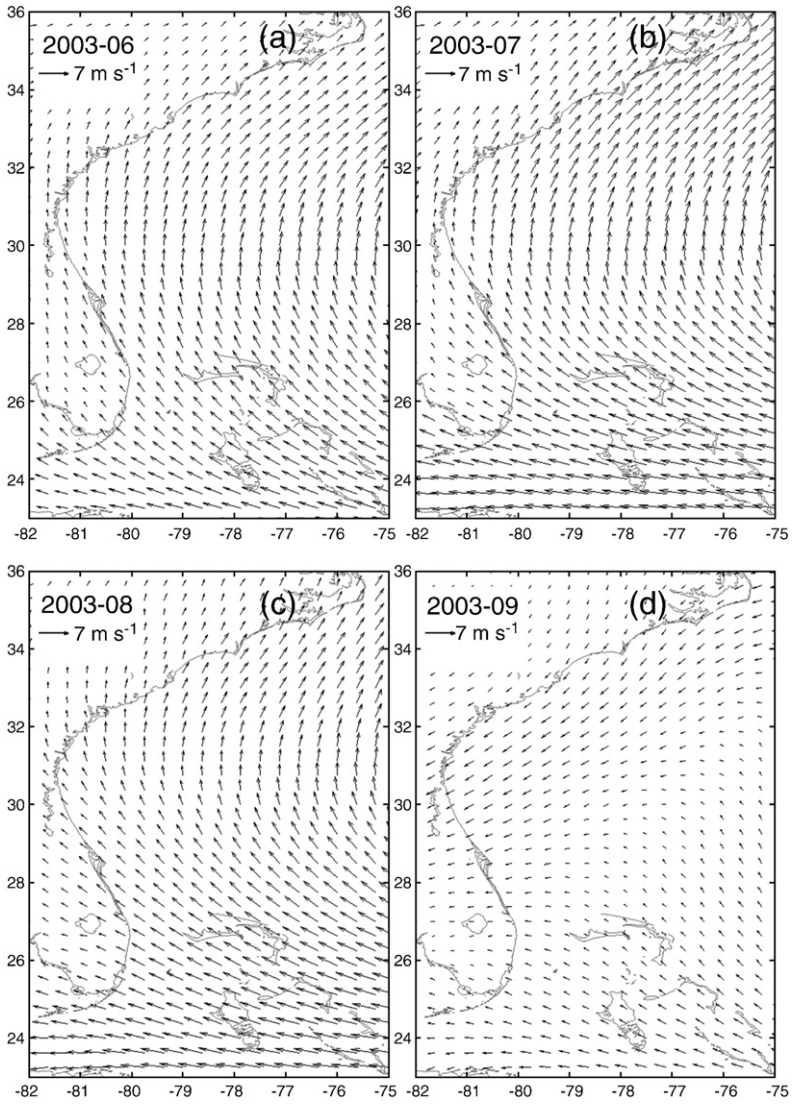

Fig. 5. Monthly mean wind vectors in (a) June, (b) July, (c) August and (d) September, 2003. Data is obtained from the North American Regional Reanalysis.

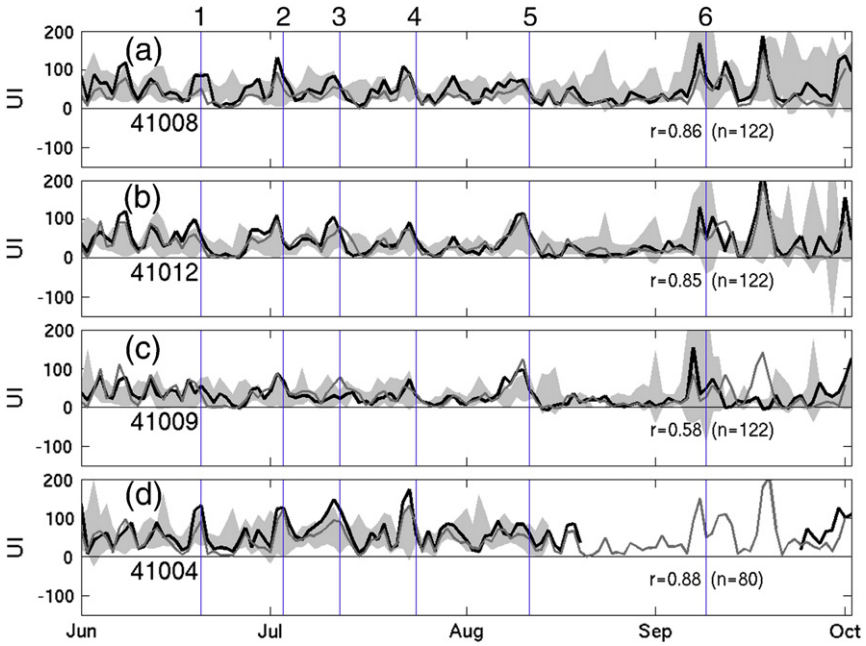

Fig. 6. Time series of daily upwelling index (*UI*, $m^3/s/100$ m) calculated from buoy (solid line) and NARR winds (gray line) for June–September 2003 at buoy (a) 41008, (b) 41012, (c) 41009 and (d) 41004. For each station, the long-term (2003–2008) standard deviation envelope is highlighted by the shaded area. Six cold wakes are denoted by vertical lines. The correlation coefficients (r) between NARR and buoy winds and their associated degrees of freedom (n) are also provided.

wind direction and the decrease of speed in September were triggered by the passage of fall extratropical frontal systems (Aretxabaleta et al. 2006).

Time series of upwelling index *UI* provided an alternative way of quantifying the variability of alongshelf wind components in summer 2003 (Fig. 6). Peaks of *UI* were found to be coincident with the cold wakes identified above, suggesting that the oscillations in the wind field were the key factor for the generations of cold wakes. We also computed *UIs* based on NARR wind field. Decent agreements between the two (correlation coefficient>0.58 at all stations) suggested that the NARR wind analysis is a realistic representation of SAB coastal wind field, lending us the confidence to use NARR meteorological forcing to drive regional circulation hindcast (see Section 3.3). How anomalous was the 2003 wind conditions can be further examined by comparing the time integral of *UI* index computed for each summer in 2002 through 2008, respectively (Fig. 7). Results at buoy 41012 for example reconfirm that the upwelling favorable winds in 2003 were indeed the most persistent over the 7-year time period.

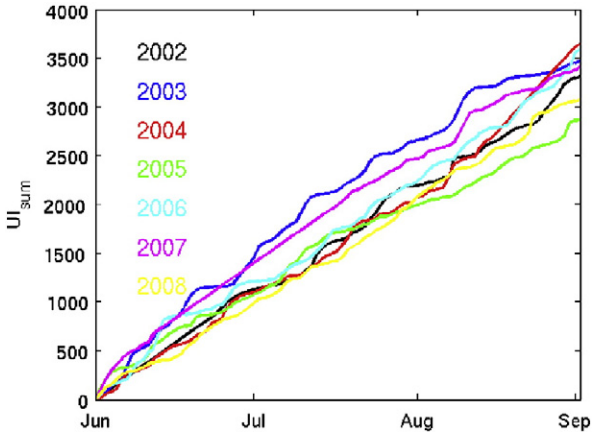

Fig. 7. Time-integrated upwelling index at buoy 41012 in summers of 2002 through 2008, respectively. Daily *UI* (shown in Fig. 6) is integrated starting on June 1 of each year.

3.3. Model hindcast

The SABGOM ROMS circulation hindcast was initialized on 1 June 2003 using the large-scale data assimilative HYCOM solutions. HYCOM fields were not available before June 2003, so our hindcast experiment could not be initialized earlier. Driven by NARR surface momentum and buoyancy forcing, coastal river runoff, and HYCOM boundary forcing, SABGOM ROMS was then integrated continuously to December 2007. For the purpose of this study, we presented model hindcast results in summer, 2003.

We began with the validation of model surface temperature field, in which we sampled modeled temperature at the nearest locations of the 4 NDBC buoys. The resulting time series comparisons (Fig. 8) showed that the model generally overestimated the cooling, but the variability is highly consistent between observed and modeled temperature. The SABGOM ROMS was skillful in reproducing occurrences and temperature variations during cold wakes, especially after mid-July (the 3rd wake). The correlation coefficients at all 4 buoy locations are all above 0.33 (the minimum threshold for r at the 95% significance level with 120 degrees of freedom is 0.13). We note that such model-data differences are in part due to the shelf water hydrographic biases in the HYCOM simulations (Chen and He, 2010), and in part due to short model spin-up period that we could not get around in this case. At the center of the cold water (i.e., locations of buoy 41008 and 41012, see Section 3.1), the discrepancy between simulated and observed temperature was less than 1 °C. A larger difference (>2 °C) was seen at buoy 41009, which is located near the shelf break east of Cape Canaveral. This is likely because the SABROM ROMS does not have sufficient resolution to resolve dynamics associated with abrupt topographic changes in that area.

Another comparison was made in terms of the GS volume transport through the Florida Straits (Fig. 9). The observational values were obtained from the cable measurement across the straits along ~27 N (section FS in Fig. 1; Baringer and Larsen, 2001), whereas the model counterpart came from the integration of simulated across-strait velocity sampled along the same transect. The observation showed that the GS volume first decreased from 35 Sv to about 30 Sv in June, then increased to 38 Sv in mid-July, before it decreased again

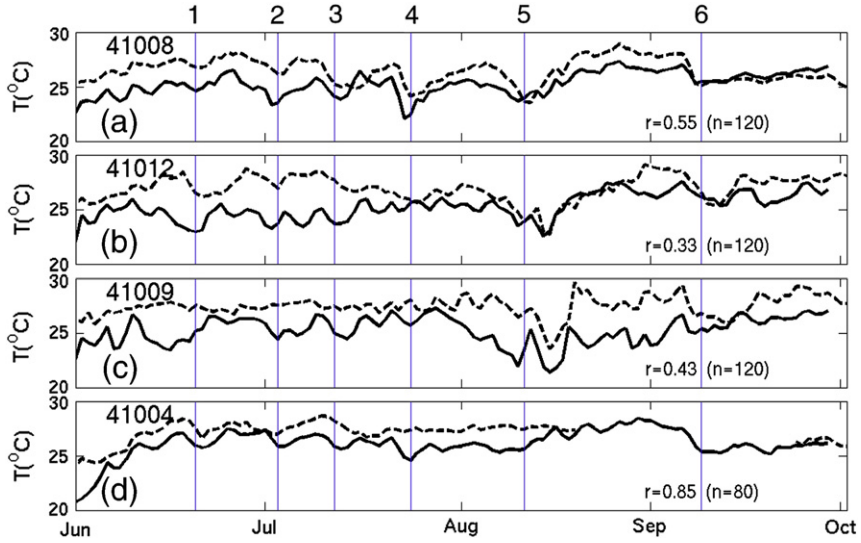

Fig. 8. Daily model-data comparisons of sea surface temperature at buoy (a) 41008, (b) 41012, (c) 41009 and (d) 41004. The correlation coefficients (r at 95% confidence level) between observed (dashed line) and simulated (solid line) temperatures and their associated degrees of freedom are provided.

in August. Such variability for the most part resides within the standard deviation envelope of the long-term mean volume transport. The simulated volume transport (the case with wind) reproduced the same observed temporal variability. The correlation coefficient between modeled and observed transport is 0.69 (the minimum threshold for r at the 95% significance level with 70 degrees of freedom is 0.23). The simulated summer mean transport is 32.7 Sv, which is consistent with the observed summer mean value of 32.4 Sv.

A comparison in the subsurface temperature distribution crossing the Georgia shelf (section G in Fig. 1) was given in Fig. 10. We used the same across-shelf temperature observations described in Aretxabaleta et al. (2006), which clearly showed the onshore transport of bottom cold water in August, 2003. Observed shelf water temperature (Fig. 10 upper two panels) ranged from 18 to 27 °C on 6 August and 16–29 °C on 27 August. The thermocline depths were located around 10–20 m. The GS intrusion defined as water colder than 18 °C below the thermocline (Atkinson, 1985) extended well onshore. The model generally reproduced these observed features (Fig. 10 middle two panels). Simulated shelf temperature ranged from 17 to 27 °C on 6 August, and from 15 to 28 °C on 27 August. While the predicted thermocline was about 5 m shallower, its spatial structures, including the mid-shelf dipping on 27 August were captured by the model.

All these model-data comparisons showed that while the nested SABGOM model was limited by its initial and open-ocean boundary conditions obtained from the large scale model, in general it was capable of capturing the spatial and temporal variabilities of SAB hydrodynamics in summer 2003, thereby allowing us to use it as a diagnostic tool to examine the physical processes important to the 2003 cold event.

4. Discussion

4.1. Effect of the wind

Bane et al. (2005, 2007) investigated intra-seasonal oscillations (ISOs) in the summer coastal upwelling system off the Oregon coast. They reported that ISOs with periods of 15–40 days were typically observed in the summertime wind stress. This wind stress variability was caused by the north–south positional oscillation of the atmospheric jet stream, and they were strong enough to modulate the coastal upwelling process. We found that the wind oscillation in the SAB similarly had a period of 10–25 days during the summer of 2003 (Fig. 11), and was highly correlated with the 3-day lagged surface temperature series ($r=0.57$ at the 95% level). We speculate that such SAB ISOs are similarly related to the large-scale atmospheric pressure systems (i.e., Azores–Bermuda High and Ohio Low or Icelandic Low). How they are generated is yet to be quantified in a future study.

The GS transport from the twin model experiment without considering wind forcing showed a reasonable correlation ($r=0.55$) with the observed values (Fig. 9). However, the resulting transport was 0.5–2 Sv less than that from the simulation with wind forcing, indicating that the summer upwelling favorable wind helped to enhance the GS volume transport through the Florida Straits.

Strong wind clearly enhanced the shelf water mixing and onshore transport in the bottom Ekman layer. The twin model experiment (Fig. 10, lower two panels) showed that without wind forcing, no surface mixed layer was formed, and on August 27, no bottom water intrusions were produced. As a result, the simulated shelf bottom temperature was

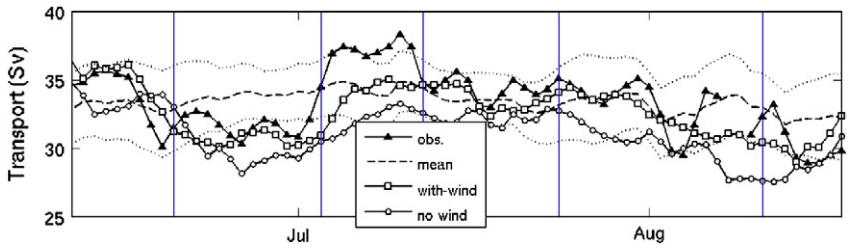

Fig. 9. Model-data comparison of the volume transport through the Florida Straits in summer 2003. Cable observed and model simulated (with/without winds) daily volume transport is depicted, along with the observed long-term (2000–2008) mean volume transport (dashed line) and its associated standard deviation envelope (dotted lines). The timings of six cold wakes are indicated by vertical lines.

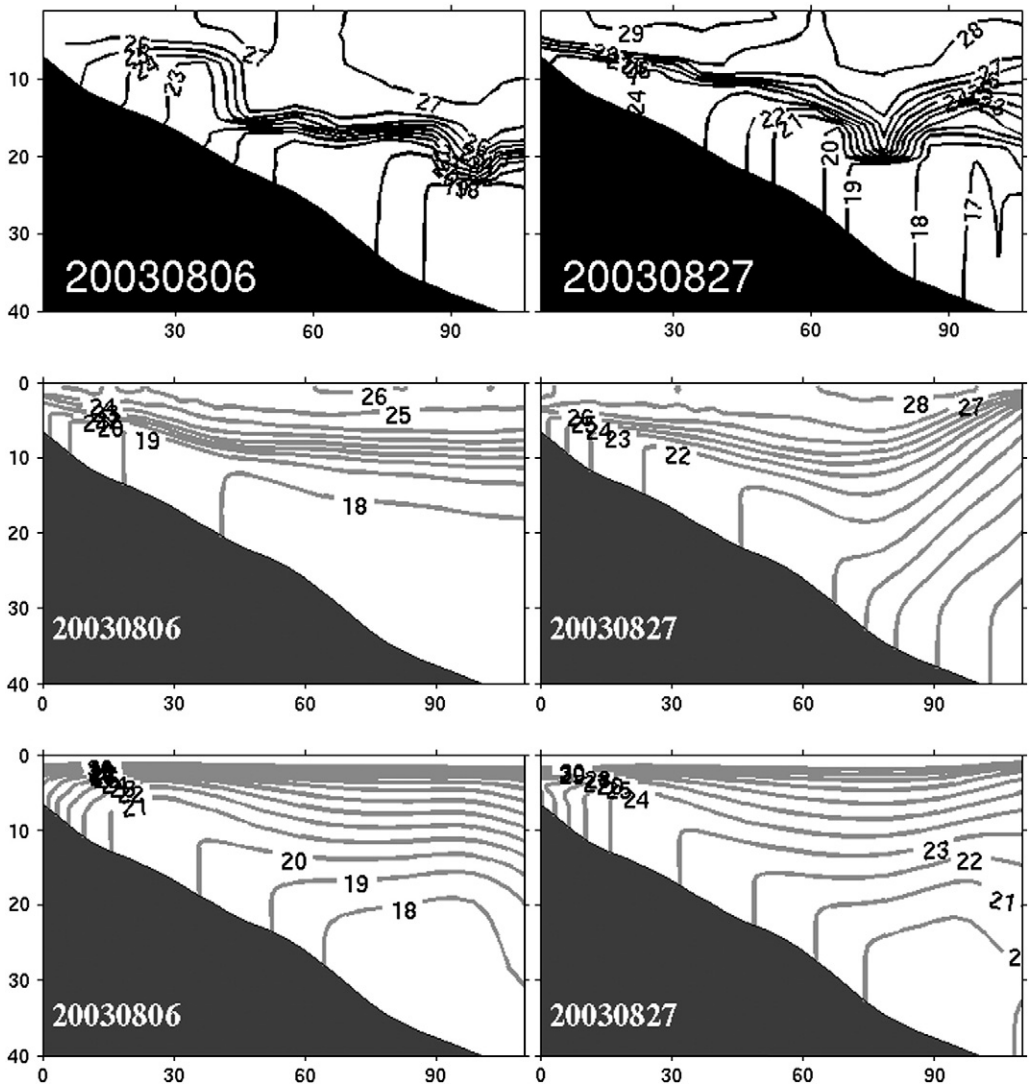

Fig. 10. Cross-shelf (G in Fig. 1) temperature transect comparisons on August 6 (left panels) and August 27 (right panels). In situ observations taken from Aretxabaleta et al. (2006) are presented in the upper panels. Simulated temperature fields from SABGOM ROMS control run (with wind forcing) are given in the middle panels, whereas simulated temperature fields from SABGOM ROMS sensitivity run (without wind forcing) are given in the lower panels.

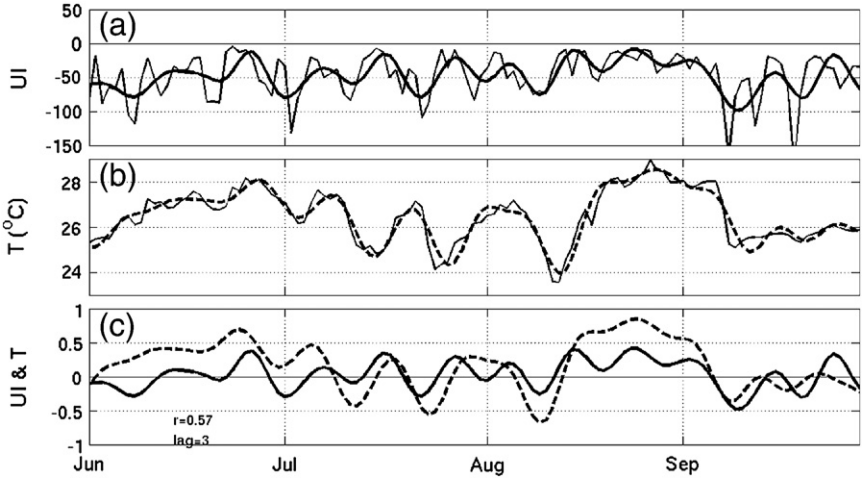

Fig. 11. (a) Daily (thin line) and 10 day low-pass filtered (thick) upwelling index and (b) daily (solid) and 10 day low-pass filtered (dashed) sea surface temperature measured by buoy 41008. For better visualization, negative sign is applied to *UI*. (c) Comparison between normalized *UI* (solid) and 3-day lagged surface temperature (dashed). The correlation coefficient between them is 0.57 at 95% confidence level.

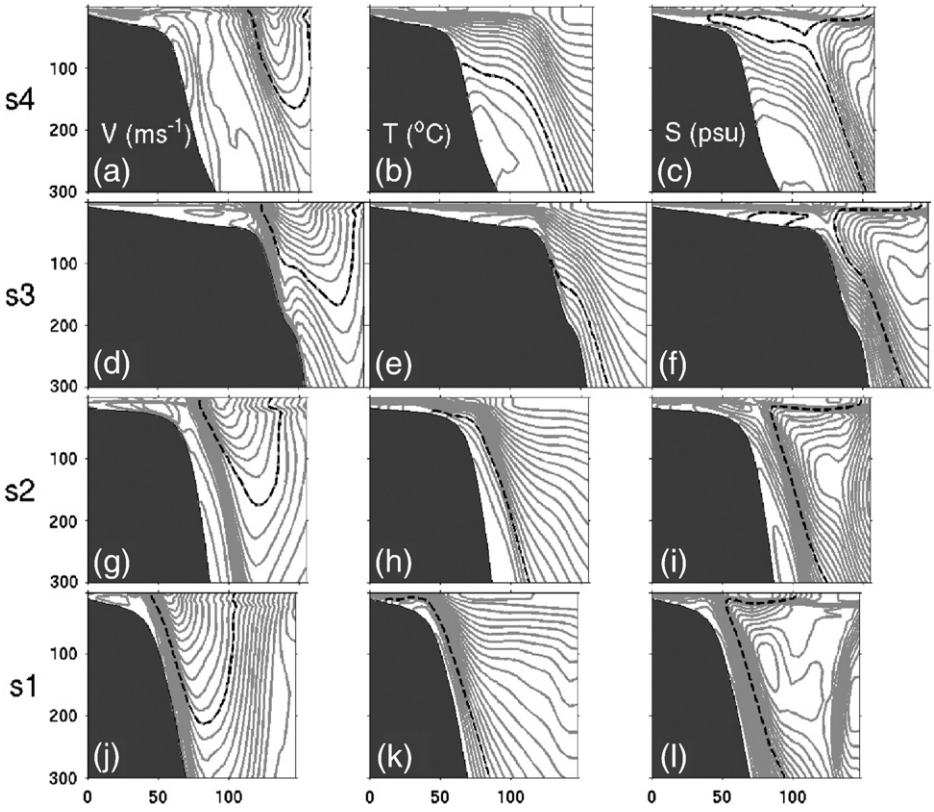

Fig. 12. Cross-shelf sections of simulated alongshore velocity (left), temperature (middle) and salinity (right) at sections S1–S4 on 11 August 2003 (the coldest anomaly). Contour intervals are 0.1 m s^{-1}, 1 °C , and 0.03 psu, respectively. Isopleths of 1.2 m s^{-1}, 12 °C and 35.6 psu are highlighted in dashed black lines, respectively. The areas >1.2 m s^{-1},<12 °C , and >35.6 psu are used to indicate the Gulf Stream core, the cold bottom water and Subtropical Underwater, respectively.

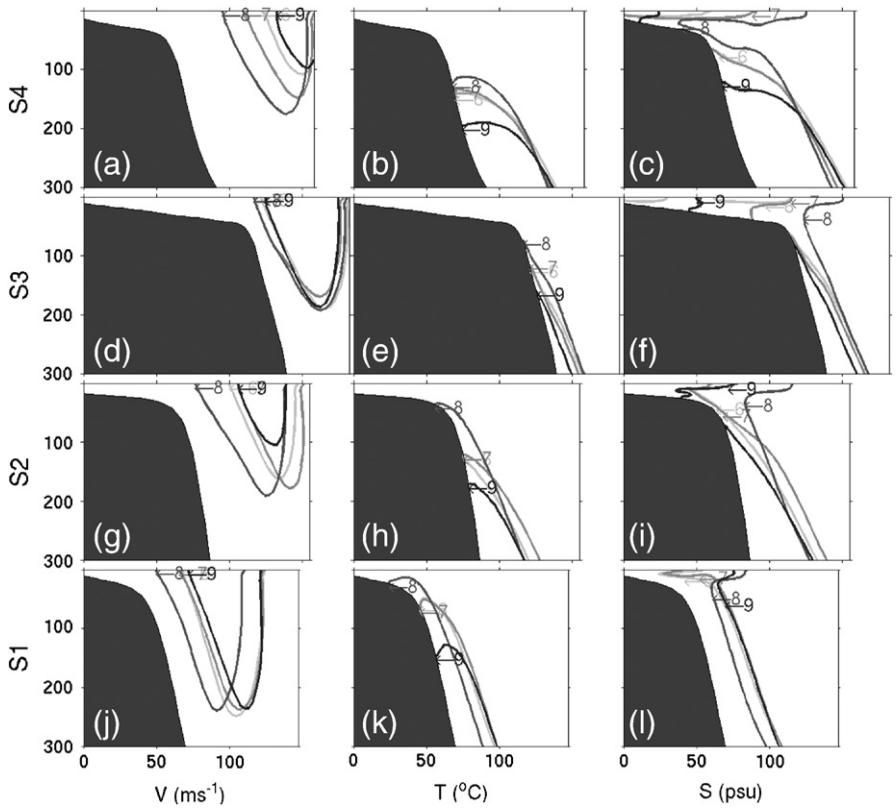

Fig. 13. Monthly positional variations (June–September) of the Gulf Stream core, the cold bottom water and Subtropical Underwater, prescribed by the contours of 1.2 m s^{-1} alongshore velocity, 12 °C isotherm, and 35.6 psu salinity, respectively. Monthly mean values are derived from SABGOM ROMS control run with wind forcing.

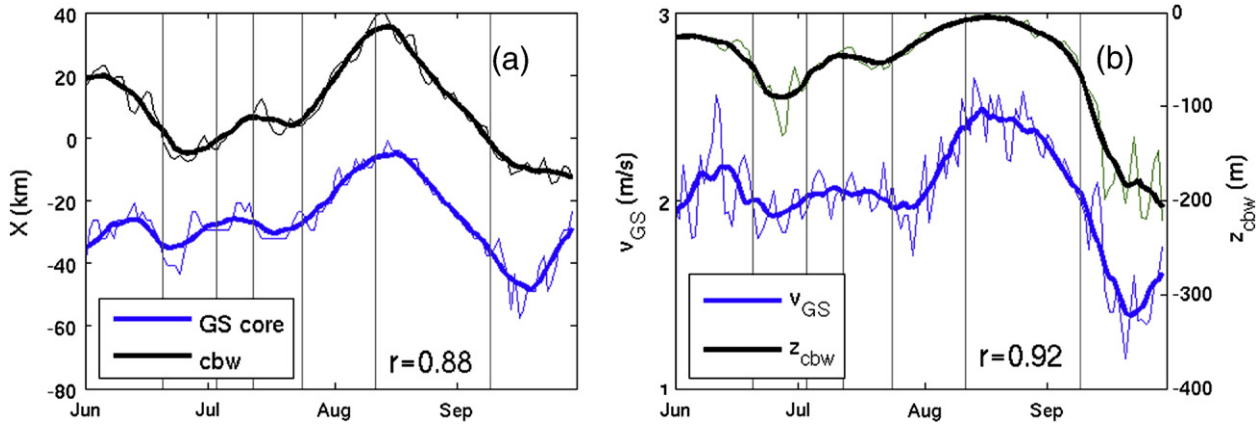

Fig. 14. Temporal variations of the cross-shelf positions of (a) the Gulf Stream core and the cold bottom water (cbw), (b) the GS core speed (v_{GS}) and the vertical location of the cold bottom water (z_{cbw}) from SABGOM ROMS control run with wind. The cross-shelf location (X) is calculated as the relative distance to the shelf break located at 50 km offshore (positive is onshore). The cross-shelf and vertical locations of the cold bottom water are based on the positions of 12 °C isotherm, whereas the GS core speed is based on the maximum alongshore velocity sampled at section S1 (shown in Fig. 12). All time series are 10 day low-pass filtered. The correlation coefficients (r at 95% confidence level) between the comparing couples are provided.

a few degrees warmer than temperature observed in situ and temperature simulated by the model control run with wind forcing.

4.2. Effects of the Gulf Stream

The spatial variation of GS and its onshore intrusion can be examined through sectional views of alongshore flow, temperature and salinity fields (Fig. 12). Major water masses appearing on the SAB slope are the GS surface water, the Subtropical Underwater (SU), and the Antarctic Intermediate Water (Atkinson, 1985). The core position and intensity of the GS water were illustrated by a swift alongshore current (1.2 m/s isopleths in Fig. 13). The GS water surface temperature ranges from 21 to 24 °C in winter, and from 27 to 29 °C in the summer. The Subtropical Underwater is characterized by a salinity maximum at about 200 m in the abyssal zone (>120 km offshore), providing a source of salt intrusion onto the shelf (as seen in Fig. 13). The cold bottom water (<18 °C) over the SAB slope can be traced from the Antarctic Intermediate Water characterized by cold waters with temperature <12 °C and the western North Atlantic Deep Water characterized by negative salinity anomaly (c.f. Read, 2001). While detailed water mass analysis is beyond the scope of this paper, we can generally define the GS core by a swift alongshore current with the speed >1.2 ms^{-1}, the cold bottom water intrusions crossing the shelf break by the 12 °C isotherms, and the salt intrusion of the Subtropical Underwater by the 35.6 psu isohalines.

On 11 August (the coldest 5th wake), the GS core was present near the shelf break and about 200 m deep along the section S1 (Fig. 12j). Downstream, the core began to weaken and shoal from sections S2 through S4. At the same time, the cold bottom water over the slope gradually migrated offshore as the latitude increased from S1 to S4. Such bottom water intrusion was most clearly seen at sections S1 and S2 (Fig. 12h, k), both are located off the east Florida coast near the Cape Canaveral. Consistent with the findings of earlier studies (e.g., Blanton et al., 1981; Atkinson et al., 1987; Lorenzzetti et al., 1987; Aretxabaleta et al., 2006), model results here confirmed that the coast region near the Cape Canaveral is prone to strong upwelling. Salt intrusions of the Subtropical Underwater were also seen at all 4 sections at the mid-depth. Different from bottom intrusions that provide colder and fresh Antarctic Intermediate Water, salt intrusions supply saline and relatively warmer water onto the shelf.

Monthly mean transects of alongshore currents, temperature and salinity clearly showed the sequential migrations of the GS core, the cold bottom water and the Subtropical Underwater (Fig. 13). In June and July, the GS core resided relatively offshore at all sections (100 km offshore at S1; 120–150 km offshore at S2–S4; Fig. 13a, d, g, i) and the depth of the core shoaled from 250 m at S1 to 180 m at S4. The upper tip of the cold bottom water was positioned at ~80 m at S1 and ~130 m at S2–S4. From July to August, the GS core approached shoreward by 20–50 km. At the same time, the cold bottom water raised up by 30–80 m. At sections S1–S2 in particular, the shoreward tips of the cold bottom water had crossed the shelf break and intruded onto the shelf (Fig. 13h, k). In September, the GS core moved offshore by 10–40 km, and the cold bottom water retreated accordingly at all sections by 80–120 m, even though onshore salt intrusions are strong at S2, S3, S4 (Fig. 13c, f, i).

The relationship of horizontal position of the GS core with the horizontal position of the cold bottom water (left panel) and the relationship of the GS intensity (i.e., the core speed) with the intrusion depth [the upper tip of the cold bottom water(CBW)] were quantified in Fig. 14. Strong correlations were found with $r = 0.88$ (0.92) between the locations of the GS core and the CBW (between the GS intensity and the intrusion depth of CBW). While we were lack of observational evidence, our multiple-year continuous ROMS hindcast (2003–2007) show that these relationships are fairly robust. Compared to other model years (2004–2007), the simulated GS path in 2003 was in a relatively more onshore position and had a larger intensity (not shown), thus allowing the cold bottom waters to intrude closer to the coast. In addition to strong upwelling favorable wind forcing, the model suggests the GS, being more intense and shoreward located, worked in concert with anomalously strong upwelling favorable wind field to produce abnormal coastal upwelling in summer 2003.

4.3. Particle trajectories

The fate of cold water intrusion can be further illustrated by Lagrangian particle trajectories simulated during the model hindcast (Fig. 15). At the beginning of each month from June through September, we released a set of numerical floats over the slope beneath the shelf edge (<60 m). Then we tracked these floats driven by simulated 3-dimensional velocity fields for a month. The resulting monthly trajectories were used to compute the percentage of water parcels (floats) that had traveled either onshore (i.e., upwelling floats) or offshore (i.e., downwelling floats). We also calculated the percentage of those drifters that finally reached the shallow shelf (<50 m) as a way to quantify the strength of on-shore transport.

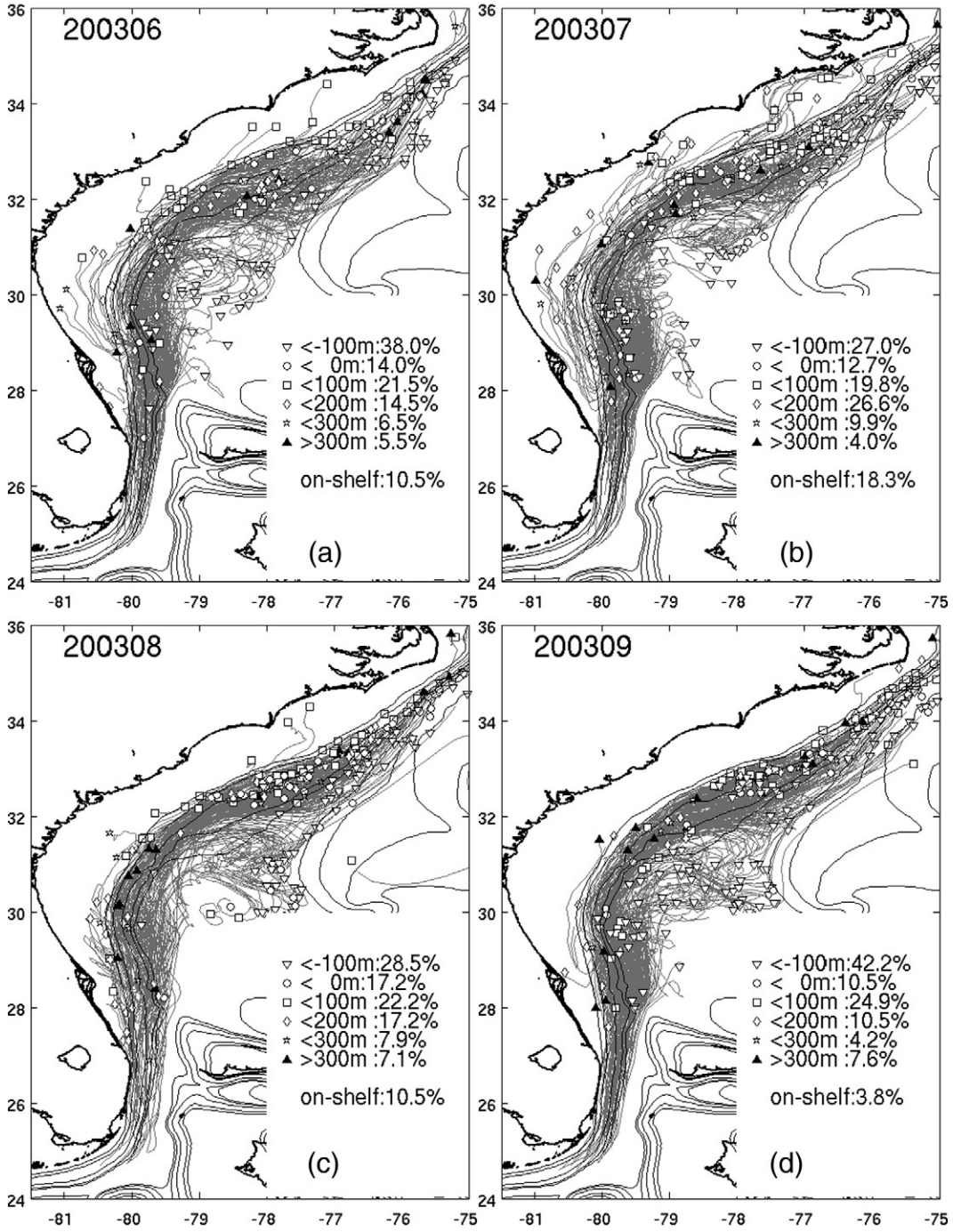

Fig. 15. Simulated float trajectories during (a) June, (b) July, (c) August, (d) September, 2003. Floats are released at the depth between 60 and 600 m over the SAB continental slope on the first day of each month and tracked for 30 days. Upwelling and downwelling floats are categorized by their vertical transport distances (<—100 m, —100–0 m, 0–100 m, 100–200 m, 200–300 m, and <300 m; positive indicates upwelling). On-shelf floats represent those whose final locations are within 50 m isobaths. The ratios of these different types of floats to the total number of float released are indicated at the lower right corner of each panel.

The percentages of upwelling floats in June, July and August were 62%, 73%, and 72%, respectively. In contrast, only 47% of drifters were upwelled in September. While only 4.2% of floats made it to the shallow shelf (<50 m) in September, 11%, 18%, and 10% of floats made to those shallow regions in June, July, and August, respectively. Drifter trajectories revealed that the cold water intrusion peaked in July. The associated strong onshore transport subsequently contributed to the coldest temperature anomaly (5th wake) observed in early August. The plan views of float trajectories further showed that the cold water intrusions in July occurred primarily in the region between 28 °N and 30 °N. Some cold water also appeared downstream off the Carolina coasts near the Charleston and Onslow Bay.

5. Summary

During the SAB cold water event of summer 2003, six cold water wakes were observed from both satellite and buoy measured sea surface temperatures. Each wake lasted about a week with an interval of roughly 2 weeks in between. Such temperature variations were similar to intra-seasonal oscillations reported for the Oregon coast by

Bane et al. (2007), but the link between oceanic and atmospheric oscillations in the SAB warrants further studies. Satellite SST demonstrated that the cold waters were centered at ~81.1 W/29.5 N near St. Augustine, Florida. After surfacing, they expanded northward and northeastward along the Florida–Georgia–Carolina coast. Examinations of long-term buoy winds showed that the upwelling favorable winds in 2003 were the strongest in the past 7 years. The upwelling index (*UI*) calculation that showed the cold wakes corresponded well with alongshore wind stress peaks ($r = 0.57$), indicating that the upwelling favorable winds played a crucial role in generating the 2003 cold water event.

Circulation hindcast experiments were performed using the primitive-equation Regional Ocean Modeling System. This regional model (SABGOM ROMS) was nested inside the 1/12° basin-scale Hybrid Coordinate Ocean Model. Realistic NARR meteorological forcing and major river runoff were considered. While the model performance was tempered by both biases in the large scale HYCOM model and the relatively short spin-up period, it generally captured temporal and spatial distributions of cold water, the variability of GS transport, and subsurface cold water intrusions. We further used the model solutions to diagnose across-shelf circulation and found significant correlations between the cold bottom water intrusion and the GS core intensity and its proximity to the shelf. Being more intensive and shoreward located in summer 2003, the GS worked in concert with strong upwelling favorable wind field to produce abnormal upwelling in 2003.

The Lagrangian drifter trackings revealed material property (e.g., nutrient) transport pathways between the deep ocean and the SAB shelf. The shelf regions off the east Florida coast and Carolina coast were the preferred destinations of upwelled water in summer 2003. Improved understanding on how the shelf-wide marine ecosystem responds to abnormal circulation scenario like the 2003 cold event clearly requires advanced observational infrastructure together with data assimilative biophysical modeling.

Acknowledgement

We are grateful for the research support NASA and ONR provided through grant NNX07AF62G and grant N00014-06-1-0739, respectively. We also acknowledge NASA GSFC for providing MODIS data that were used to construct DINEOF SST fields, NCEP NARR for providing surface meteorological data, NDBC for providing buoy observations, NOAA AOML for providing cable data of Gulf Stream transport, and USGS for providing river flow used in this research. Dr. M. Li and Mr. T. Mile are acknowledged for their assistance in implementing the SABGOM circulation modeling and processing cloud-free DINOEOF SST fields. We thank Dr. A. Aretxabaleta and B. Blanton for providing SAB hydrographic observations and Dr. J. Bane for helpful discussions on intra-seasonal oscillations. We are indebted to two anonymous reviewers for their constructive comments and suggestions.

References

Aretxabaleta, A., Nelson, J.R., Blanton, J.O., Seim, H.E., Werner, F.E., Bane, J.M., Weisberg, R., 2006. Cold event in the South Atlantic Bight during summer of 2003: anomalous hydrographic and atmospheric conditions. J. Geophys. Res. 111, C06007. doi:10.1029/2005JC003105.

Aretxabaleta, A., Blanton, B.O., Seim, H.E., Werner, F.E., Nelson, J.R., Chassignet, E.P., 2007. Cold event in the South Atlantic Bight during summer of 2003: model simulations and implications. J. Geophys. Res. 112, C05022. doi:10.1029/2006JC003903.

Atkinson, L.P., 1985. Hydrography and nutrients of the Southeastern U.S. Continental Shelf. In: Atkinson, L.P., et al. (Ed.), Oceanography of the Southeastern U.S. Continental Shelf. Coastal and Estuarine Sciences, 2. AGU, Washington D.C, pp. 77–92.

Atkinson, L.P., Lee, T.N., Blanton, J.O., Paffenhöfer, G.A., 1987. Summer upwelling on the southeastern continental shelf of the USA during 1981: hydrographic observations. Progr. Oceanogr. 19, 231–266.

Atkinson, L.P., Menzel, D.W., 1985. Introduction: oceanography of the Southeast United States Continental Shelf. In: Atkinson, L.P., et al. (Ed.), Oceanography of the Southeastern U.S. Continental Shelf. : Coastal and Estuarine Sciences, 2. AGU, Washington D.C, pp. 1–9.

Bane, J.M., Spitz, Y.H., Letelier, R.M., Peterson, W.T., 2007. Jet stream intraseasonal oscillations drive dominant ecosystem variations in Oregon's summertime coastal upwelling system. PNAS 104, 13262–13267. doi:10.1073/pnas.0700926104.

Bane, J.M., Levine, M.D., Samelson, R.M., Haines, S.M., Meaux, M.F., Perlin, N., Kosro, P.M., Boyd, T., 2005. Atmospheric forcing of the Oregon coastal ocean during the 2001 upwelling season. J. Geophys. Res. 110, C10S02. doi:10.1029/2004JC002653.

Baringer, M.O., Larsen, J.C., 2001. Sixteen years of Florida Current Transport at 27 N. Geophysical Research Letters 28 (16), 3,179–3,182.

Blanton, J.O., Amft, J.A., Lee, D.K., Riordan, A., 1989. A wind stress and heat fluxes observed during winter and spring 1986. J. Geophys. Res. 94, 10686–10698.

Blanton, B.O., Aretxabaleta, A.L., Werner, F.E., Seim, H., 2003a. Monthly climatology of the continental shelf waters of the South Atlantic Bight. J. Geophys. Res. 108 (C8), 3264. doi:10.1029/2002JC001609.

Blanton, B.O., Aretxabaleta, A., Werner, F.E., Seim, H.E., 2003b. Monthly climatology of the continental shelf waters of the South Atlantic Bight. J. Geophys. Res. 108 (C8), 3264. doi:10.1029/2002JC001609.

Blanton, B.O., Werner, F.E., Seim, H., Luettich, R.A., Lynch, D.R., Smith, K.W., Voulgaris, G., Bingham, F.M., Way, F., 2004. Barotropic tides in the South Atlantic Bight. J. Geophys. Res. 109, C12024. doi:10.1029.2004JC002455.

Blanton, J.O., Atkinson, L.P., Pietrafesa, L.J., Lee, T.N., 1981. The intrusion of Gulf Stream Water across the continental shelf due to topographically-induced upwelling. Deep Sea Res. 28A, 393–405.

Brooks, D.A., Bane Jr., J.M., 1978. Gulf Stream deflection by a bottom feature off Charleston. SC. J. Phys. Oceanogr. 474, 1225–1226.

Chassignet, E.P., Smith, L.T., Halliwell, G.R., Bleck, R., 2003. North Atlantic simulations with the Hybrid Coordinate Ocean Model (HYCOM): impact of the vertical coordinate choice, reference pressure, and thermobaricity. J. Phys. Oceanogr. 33, 2504–2526.

Chao, S.Y., Janowitz, G.S., 1979. The effect of a localized topographic irregularity on the flow of a boundary current along the continental margin. J. Phys. Oceanogr. 9, 900–910.

Chen, K., He, R., 2010. Numerical investigation of the Middle Atlantic Bight Shelfbreak Frontal Circulation Using a high-resolution ocean hindcast model. J. Phys. Oceanogr. 40, 949–964.

Dewar, W.K., Bane Jr., J.M., 1985. Subsurface energetics of the Gulf Stream near the CB. J. Phys. Oceanogr. 15, 1771–1789.

Hamilton, P., 1987. Summer upwelling on the southeastern continental shelf of the USA during 1981: the structure of the shelf and Gulf Stream motions in the Georgia Bight. Progr. Oceanogr. 19, 329–351.

Haidvogel, D.B., Arango, H., Budgell, W.P., Cornuell, B.D., Curchitser, E., Di Lorenzo, E., Fennel, K., Geyer, W.R., Hermann, A.J., Laneroll, L., Levvi, J., McWilliams, J.C., Moore, A.J., Powell, T.M., Shchepetkin, A.F., Sherwood, C.R., Signell, R.P., Warner, J.C., Wilkin, J., 2008. Ocean forecasting in terrain-following coordinates: formulation and skill assessment of the Regional Ocean Modeling System. J. Comp. Physics 227, 3595–3624.

Hofmann, E.E., 1981. Plankton dynamics on the outer southeastern U.S. continental shelf. Part III: A coupled physical–biological model. J. Mar. Res. 46, 919–946.

Janowitz, G.S., Pietrafesa, L.J., 1982. The effect of alongshore variation in bottom topography on a boundary current. Cont. Shelf Res. 1, 123–141.

Klinck, J.M., Pietrafesa, L.J., Janowitz, G.S., 1981. Continental shelf circulation induced by a moving, localized wind stress. J. Phys. Oceanogr. 11, 836–848.

Large, W.G., Pond, S., 1981. Open ocean momentum flux measurements in moderate to strong winds. J. Phys. Oceanogr. 11, 324–336.

Lee, T.N., Atkinson, L.P., 1983. Low-frequency current and temperature variability from Gulf Stream frontal eddies and atmospheric forcing along the southeast U.S. outer continental shelf. J. Geophys. Res. 88, 4541–4567.

Lee, T.N., Kourafalou, V.H., Wang, J.D., Ho, W.J., Blanton, J.O., Atkinson, L.P., Pietrafesa, L.J., 1985. Shelf circulation from Cape Canaveral to Cape Fear during winter. Oceanography of the Southeastern U. S. Continental Shelf, Coastal Estuarine Stud., vol. 2, edited by L. P. Atkinson et al. AGU, Washington, D. C, pp. 33–62.

Lee, T.N., Pietrafesa, L.J., 1987. Summer upwelling on the southeastern continental shelf of the U.S.A. during 1981: circulation. Progr. Oceanogr. 19, 267–312.

Lee, T.N., Atkinson, L.P., Legekis, R., 1981. Observations of a Gulf Stream frontal eddy on the Georgia continental shelf, April 1977. Deep Sea Res. 28, 347–378.

Lee, T.N., Yoder, J.A., Atkinson, L.P., 1991. Gulf Stream frontal eddy influence on productivity of the southeast U.S. continental shelf. J. Geophys. Res. 96, 22,191–22,205.

Lorenzzetti, J., Wang, J.D., Lee, T.N., 1987. Summer upwelling on the southeastern continental shelf of the U.S.A. during 1981: circulation modelling. Progr. Oceanogr. 19, 313–327.

Miles, T.N., He, R., Li, M., 2009. Characterizing the South Atlantic Bight seasonal variability and cold-water event in 2003 using a daily cloud-free SST and chlorophyll analysis. Geophys. Res. Lett. 36, L02604. doi:10.1029/2008GL036396.

Pietrafesa, L., Blanton, J.O., Atkinson, L.P., 1978. Evidence for deflection of the Gulf Stream at the Charleston Rise. Gulf Stream 4, 9, 3, 6–7.

Read, J.F., 2001. CONVEX-91: water masses and circulation of the Northeast Atlantic subpolar gyre. Progress In Oceanography 48 (4), 461–510.

Rooney, D.M., Janowitz, G.S., Pietrafesa, L.J., 1978. A simple model of deflection of the Gulf Stream by the Charleston rise. Gulf Stream 4 (11), 3–7.

Shchepetkin, A.F., McWilliams, J.C., 2005. The Regional Ocean Modeling System: a split-explicit, free-surface, topography-following-coordinate oceanic model. Ocean Modeling 9/4, 347–404. doi:10.1016/j.ocemos.2004.08.002.

Schwing, F.B., Pickett, M.H., 2004. Comment on "Anomalous Cold Water Detected Along Mid-Atlantic Coast". *Eos Trans.* AGU 85 (51). doi:10.1029/2004EO510004.

Schwing, F.B., M. O'Farrell, J. Steger and K. Baltz. (1996), Coastal upwelling indices, West coast of North America, 1946–1995. U.S. Dept. of Commerce, NOAA Tech. Memo. NOAA-TM-NMFS-SWFC-231, 207 pp.
Signorini, S.R., McClain, C., 2007. Large-scale forcing impact on biomass variability in the South Atlantic Bight. Geophys. Res. Lett. 34, L21605. doi:10.1029/2007GL03121.
Werner, F. E., J. O. Blanton, D. R. Lynch, and D. K. Savidge (1993), A numerical study of the continental shelf circulation of the U.S. South Atlantic Bight during the autumn of, 1987. cont. Shelf Res. 13, 871–997.
Xie, L., Liu, X., Pietrafesa, L.J., 2007. Effect of bathymetric curvature on Gulf Stream instability in the vicinity of the Charleston Bump. J. Phys. Oceanogr. 37, 452–475.
Yuan, D., 2006. Dynamics of the cold-water event off the Southeast Coast of the United States in the summer of 2003. J. Phys. Oceanogr. 36, 1912–1927.